Observation of the parametric-modulational instability between the drift-wave fluctuation and azimuthally symmetric sheared radial electric field oscillation in a cylindrical laboratory plasma

Yoshihiko Nagashima,[1,a)] Sanae-I. Itoh,[1] Shunjiro Shinohara,[2] Masayuki Fukao,[3] Akihide Fujisawa,[4] Kenichiro Terasaka,[2] Yoshinobu Kawai,[1] George R. Tynan,[5] Patrick H. Diamond,[6] Masatoshi Yagi,[1] Shigeru Inagaki,[1] Takuma Yamada,[1] and Kimitaka Itoh[4]

[1]*RIAM, Kyushu University, Kasuga, Fukuoka 816-8580, Japan*
[2]*IGSES, Kyushu University, Kasuga, Fukuoka 816-8580, Japan*
[3]*Uji, Kyoto 611-001, Japan*
[4]*National Institute for Fusion Science, Toki, Gifu 509-5292, Japan*
[5]*CER, University of California, San Diego, La Jolla, California 92093-0417, USA*
[6]*CASS, University of California, San Diego, La Jolla, California 92093-0424, USA*

(Received 1 December 2008; accepted 14 January 2009; published online 20 February 2009)

Observation of the parametric-modulational interaction between the drift-wave fluctuation (7–8 kHz) and azimuthally symmetric sheared radial electric field structure (~0.4 kHz) in a cylindrical laboratory plasma is presented. Oscillation of the sheared radial electric field is synchronized at modulations of the radial wave number and Reynolds stress per mass density of the drift-wave spectrum. Bispectral analysis at the location where the sheared radial electric field has finite radial wave numbers shows that nonlinear energy transfers from the drift wave to the sheared radial electric field occur. Nonlocal energy transfers of fluctuations via "channel of the azimuthally symmetric sheared radial electric field" in spectral space as well as real space are discovered. © *2009 American Institute of Physics*. [DOI: 10.1063/1.3078075]

Study on nonlinear dynamics of plasma turbulence is important for understanding turbulence saturation and transport.[1] Recent theoretical progresses have highlighted importance of secondary/tertiary instabilities excited by microscale turbulence. In particular, zonal flows, azimuthally symmetric bandlike shear flows, could be a secondary instability driven by microscale fluctuations.[2–4] Zonal flows can also reduce turbulence and transport[5] and could have a large contribution to turbulence saturation. Therefore, nonlinear processes among zonal flows/fields and microscale turbulence have been studied experimentally in fusion plasma community.[6–17] Bicoherence analysis has contributed to the studies. In addition, studies of nonlinear coupling between secondary instabilities with finite poloidal wave numbers and microscale fluctuations have been also performed.[18] In the next stage, beyond the simple bicoherence analysis,[19] experimental studies on detailed mechanism of such nonlinear processes are required. For instance, in the case that microscale fluctuations excite nonlinearly azimuthally symmetric structure with finite radial wave numbers, the nonlinear interaction occurs through modulation of the radial wave number rather than that of the poloidal wave number. This process is the central mechanism under which zonal flows is driven by the drift wave (DW), named parametric-modulational instability (PMI).[2,17] In the PMI, the energy transfer directions are considered not to be unique in spectral space[20] and real space.[21] Therefore, studies on the energy transfer direction among fluctuations have progressed.[22–24] However, there are many tasks for clarifying experimentally the mechanism of the PMI. In this article, we present an experimental identification of the PMI between azimuthally symmetric sheared radial electric field structure (~0.4 kHz) and DW fluctuation (7–8 kHz) in a cylindrical laboratory plasma. In particular, we emphasize observation of the radial wave number modulation and nonlinear/nonlocal energy transfer in the PMI. First, we briefly describe experimental setups and observed quadratic spectra. Next, we demonstrate modulations of the radial wave number and Reynolds stress (RS) per mass density of the DW spectrum. Then, we track nonlinear energy transfers in frequency domain by use of bispectral analysis and identify the PMI in the spectrum. Finally, we report discovery of nonlocal energy transfer of fluctuations via the sheared radial electric field in real and spectral spaces.

Experiments were conducted on a linear device, the large mirror device,[25] and experimental conditions are reported in Ref. 26. Fluctuations are mainly measured with a Reynolds stress probe (RSP) located 60 cm ($Z=60$ cm) away from the end of the vessel (source side, $Z=0$ where Z means the axial coordinate). The RSP head houses five electrodes.[26] One electrode is used for the ion saturation current fluctuation ($\tilde{I}_{i,\mathrm{sat}}$) measurement. The other four electrodes are used for the floating potential fluctuation ($\tilde{\Phi}_f$) measurement. We used three $\tilde{\Phi}_f$ for obtaining RS $-\langle\tilde{u}_r\tilde{u}_\theta\rangle=\langle\tilde{E}_\theta\tilde{E}_r/B^2\rangle$ (4–40 kHz). The poloidal electric field fluctuation $\tilde{E}_\theta=(\tilde{\Phi}_{f,3}-\tilde{\Phi}_{f,1})/d_\theta$ and the poloidal wave number k_θ were measured by a pair of electrodes (1 and 3 in Ref. 26) with the poloidal separation $d_\theta=4.4$ mm. The radial electric field fluctuation $\tilde{E}_r=[\tilde{\Phi}_{f,2}-(\tilde{\Phi}_{f,3}+\tilde{\Phi}_{f,1})/2]/d_r$ and the radial wave number k_r were obtained by using electrode 2 and the average of electrodes 1

a)Electronic mail: nagashima@k.u-tokyo.ac.jp.

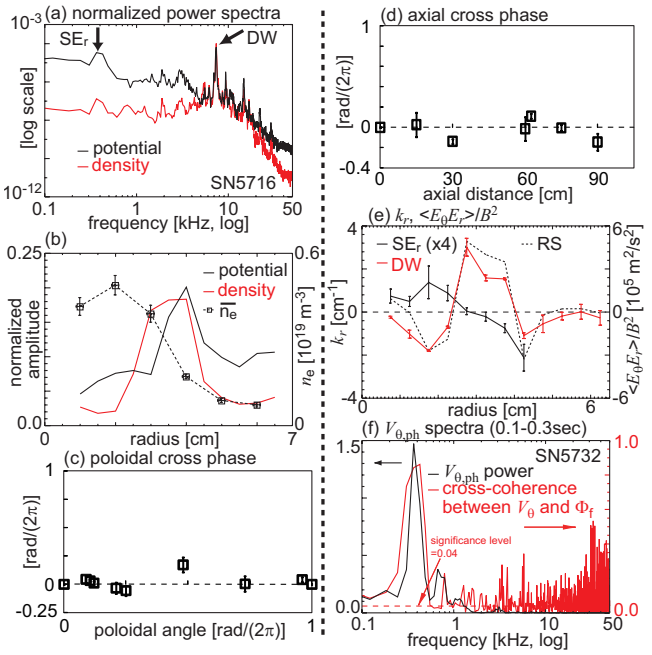

FIG. 1. (Color) Autopower spectra of $\tilde{\Phi}_f/\overline{T_e}$ (black) or $\tilde{I}_{i,\mathrm{sat}}/\overline{I}_{i,\mathrm{sat}}$ (red). (b) Radial profiles of $\tilde{\Phi}_f/\overline{T_e}$ (black), $\tilde{I}_{i,\mathrm{sat}}/\overline{I}_{i,\mathrm{sat}}$ (red), and n_e (dashed line). Profiles of (c) poloidal and (d) axial cross phase of the SE$_r$. (e) Radial profiles of k_r of the SE$_r$ (black) and DW (red), and the RS (dashed line). (f) Autopower spectrum of $\tilde{V}_{\theta,\mathrm{ph}}$ (black) or squared cross coherence between $\tilde{V}_{\theta,\mathrm{ph}}$ and $\tilde{\Phi}_f$ (red). Figures (a), (b), (e), and (f) are partially quoted from Ref. 26.

and 3, where the d_r=5 mm is the radial separation between them. We also measure poloidal phase velocity of fluctuations $\tilde{V}_{\theta,\mathrm{ph}}$ by using time delay estimation (TDE).[16] The sign of B is positive in the right-handed coordinate, so that the positive RS drives the positive potential. In addition to the RSP, a number of Langmuir probes are installed for azimuthal/axial cross-phase measurements of the potential fluctuations. The Langmuir probes have one or two electrodes, respectively, and are radially movable. The probes arranged azimuthally are located at the poloidal angles of −7° to 263° at Z=90 cm. The probes arranged axially are installed at Z=15–105 cm at the poloidal angle of 90°. Unless stated in figures, the length of the data window for fast Fourier transform (FFT) in spectral analyses is 16 384. Error estimation is based on the statistical significance of spectral analysis and the variance in a number of discharges (≥5 shots). Coherences and bicoherences are considered in the error estimation.

Linear dispersion relations of observed fluctuations are described in Ref. 26. In following three paragraphs and Fig. 1, we briefly describe quadratic spectra. Figure 1(a) shows the normalized autopower spectra ($\tilde{\Phi}_f/\overline{T_e}$ and $\tilde{I}_{i,\mathrm{sat}}/\overline{I}_{i,\mathrm{sat}}$) at the radial position r=3.5 cm where the density gradient scale is short [Fig. 1(b)]. Comparing $\tilde{\Phi}_f$ with $\tilde{I}_{i,\mathrm{sat}}$, fluctuations in the range of 4–20 kHz hold as $\tilde{\Phi}_f/\overline{T_e} \sim \tilde{I}_{i,\mathrm{sat}}/\overline{I}_{i,\mathrm{sat}}$. A spectral peak is observed at 7–8 kHz (the fundamental mode, DW), and its higher harmonics are found. In addition, another spectral peak at about 0.4 kHz has the condition that $\tilde{I}_{i,\mathrm{sat}}/\overline{I}_{i,\mathrm{sat}} \ll \tilde{\Phi}_f/\overline{T_e}$ (sheared radial electric field SE$_r$). Figure 1(b) shows the radial profiles of the normalized fluctuation level of the DW (integrated in 4–10 kHz) and the stationary electron density $\overline{n_e}$. The $\tilde{I}_{i,\mathrm{sat}}/\overline{I}_{i,\mathrm{sat}}$ of the DW has a maximum at r=3–4 cm near the steep n_e gradient region.

We estimate poloidal and axial mode numbers (m,n) at r=4 cm by use of the cross-phase analysis [Figs. 1(c) and 1(d)]. The m and n of the SE$_r$ show that $|m|,|n|<0.2$ and are consistent with (m,n)=0 (no radial $\mathbf{E}\times\mathbf{B}$ velocity). Figure 1(e) shows profiles of the k_r of the DW and SE$_r$. The signs of the k_r of the DW change at $r\sim$2.4 cm, where the mean RS profile has large gradients. The polarity of the k_r of the SE$_r$ inverts around the location where the amplitude of the DW has a maximum. We observed counterpropagating SE$_r$ with opposite directions, and they propagate toward the location where the SE$_r$ has a zero k_r (zero $k_r^{\mathrm{SE}_r}$ location). Intensities of $\tilde{\Phi}_f/\overline{T_e}$ of the SE$_r$ are uniform at $r<$4.5 cm, even at the zero $k_r^{\mathrm{SE}_r}$ location. Therefore, the SE$_r$ at the zero $k_r^{\mathrm{SE}_r}$ location has a signature of a standing wave. In the radial location where k_r of the SE$_r$ has a finite value, a spectral peak of $\tilde{V}_{\theta,\mathrm{ph}}$ at the SE$_r$ frequency is observed by using TDE analysis, as shown in Fig. 1(f) (black, at r=2.5 cm). The 512 μs time window (longer than the cycle of 7–8 kHz DW and shorter than the cycle of 0.4 kHz SE$_r$) was used in the time-resolved cross-correlation analysis. The $\tilde{V}_{\theta,\mathrm{ph}}$ at the SE$_r$ frequency has the significant coherence with potential [red in Fig. 1(f)], indicating the SE$_r$ is associated with poloidal phase and/or group velocity oscillations of the DW.

The DW propagates in the electron diamagnetic drift direction with (m,n)=(3–5,2–3). The interpretation of resistive drift instability is discussed in Ref. 27 and references therein. Not considering the effect of the Doppler shift of dc electric field, the DW frequency is $f_{\mathrm{DW,th}}=\omega^*/(2\pi)/(1+k_\perp^2\rho_s^2)$, where $\omega^*=k_\theta T_e/eB\lambda_n$ and λ_n is the density gradient scale length. We calculate $f_{\mathrm{DW,th}}$ at $r\sim$3.5 cm where the radial distribution of $\tilde{I}_{i,\mathrm{sat}}/\overline{I}_{i,\mathrm{sat}}$ has a maximum. For the experimental parameters, m=3–5, T_e=3.1 eV, λ_n=1.3 cm, and k_r=1.8 cm are used (measured at 0.3 s from the beginning of the discharge). The $f_{\mathrm{DW,th}}$=6.2–8.3 kHz is obtained and is consistent with the observed peak frequency of 7–8 kHz. (Precise Doppler shift by dc electric field will be measured in the future.)

In the DW-zonal flow system, the PMI can transfer energies of fundamental DW into DW quasimodes, azimuthally symmetric zonal flows, and/or general Kelvin–Helmholtz modes with finite poloidal wave numbers ($m\neq0$, $k_r\neq0$).[2,27] We focus our scope of this paper on the nonlinear process between the azimuthally symmetric sheared radial electric field and the DW fluctuation in the radial wave number space. The actual nonlinear interaction among them occurs through a modulation of k_r rather than k_θ of the waves.[2] Figures 2(a) and 2(c) demonstrate time evolutions of wave numbers (k_r and k_θ) of the DW at two different radial locations. The wave numbers are measured by short-time two-point cross-phase analysis, which is affected by information of both wave numbers and phase velocities of fluctuation (v_{ph}). The k_r of the DW oscillates with the amplitude of 0.2–0.3 cm^{-1} at both locations. The SE$_r$ has an $m\sim0$ and is not associated with radial $\mathbf{E}\times\mathbf{B}$ flow. In contrast, modula-

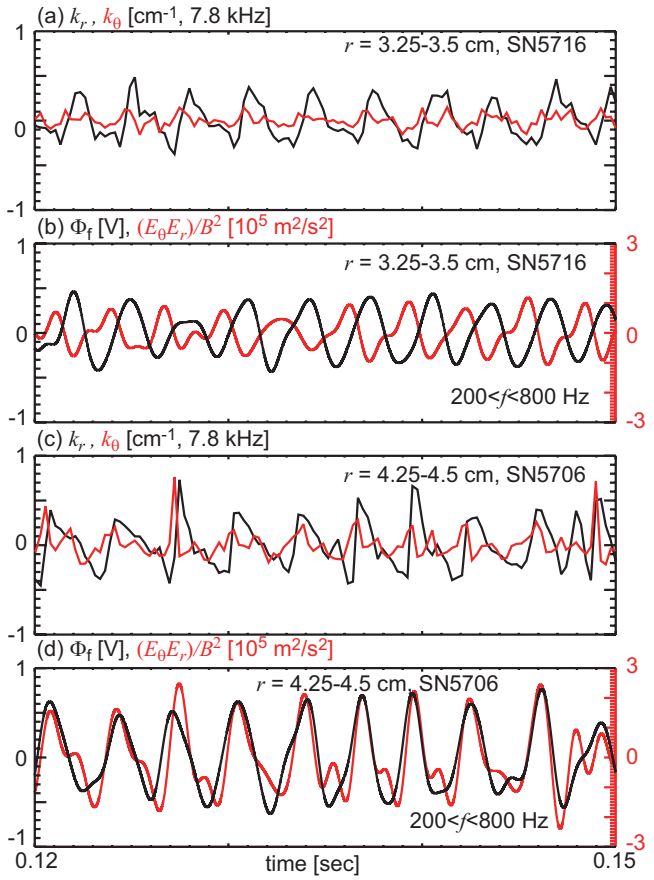

FIG. 2. (Color) Modulational instabilities [SN 5716, (a) and (b)] at $r=3.25-3.5$ cm and [SN 5706, (c) and (d)] at $r=4.25-4.5$ cm. [(a) and (c)] The $k_r(t)$ and $k_\theta(t)$ obtained by two-point cross-phase analysis. (The length of a data window for FFT is 512 μs and no ensemble average is performed.) [(b) and (d)] The $\tilde{\Phi}_f(t)$ of the SE$_r$ and modulation of the RS of the DW ($0.2<f<0.8$ kHz).

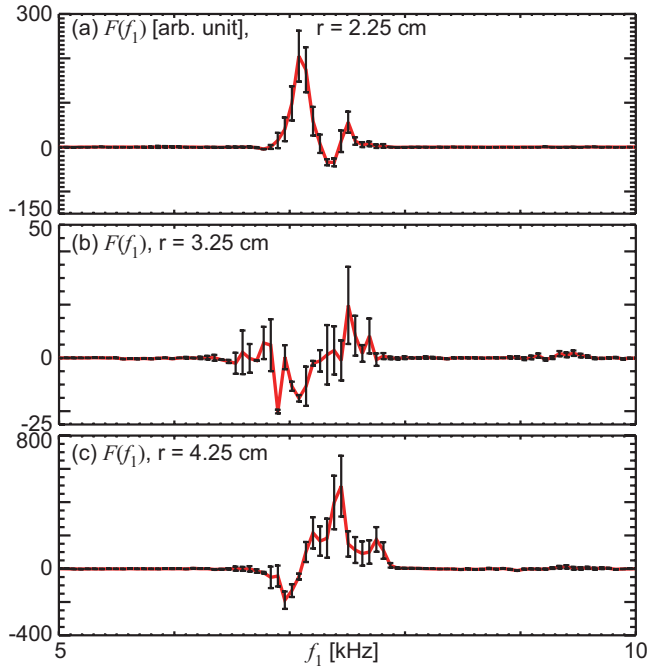

FIG. 3. (Color) Nonlinear energy transfer function $F(f_1)\equiv[k_r(f_1)+k_r(f_3-f_1)]\Im\langle\tilde{E}_\theta(f_1)\tilde{E}_r(f_3-f_1)\tilde{E}^*_{r,\mathrm{SE}_r}(f_3)\rangle$ between the DW and SE$_r$ measured at three different radial locations ($f_3=366$ Hz, and $f_3=f_1+f_2$). The cross coherence and cross bicoherence are used for error estimation. The functions are measured at (a) $r=2.25$, (b) 3.25, or (c) 4.25 cm, respectively.

tion of k_θ is less than 0.07 cm^{-1}, i.e., $\delta m<1$, at $r=3.25-3.5$ cm, and k_θ is affected very little. A weak modulation ($|\delta m|\lesssim 1$) is observed at $r=4.25-4.5$ cm, but this could be a contamination of $\tilde{V}_{\theta,\mathrm{ph}}$ of the SE$_r$ in laboratory frame. Therefore it is evident that the k_r of the DW is modulated at the SE$_r$ frequency, and we can conclude that the DW front is periodically bent by the SE$_r$ as has been discussed in many theories. Figures 2(b) and 2(d) show time evolutions of $\tilde{\Phi}_f/\overline{T_e}$ of the SE$_r$ and RS. Based on the vorticity equation $\partial_t\Delta\tilde{\Phi}_{\mathrm{SE}_r}/B=\partial_{rr}\langle\tilde{E}_\theta\tilde{E}_r\rangle/B^2-\mu\Delta\tilde{\Phi}_{\mathrm{SE}_r}/B$,[6,7] the phase relationship between the potential and turbulence RS suggests nonlinear energy transfer between them, where $\Delta\tilde{\Phi}_{\mathrm{SE}_r}$ is the vorticity of the SE$_r$ and μ is the damping rate of the $\tilde{\Phi}_{\mathrm{SE}_r}$. The observed phase relationship between the SE$_r$ and RS varies with radius. The SE$_r$ and RS are out of phase at $r=3.25$ cm. On the contrary, the SE$_r$ is in phase with the RS at $r=4.25$ cm, suggesting that the DW generates the SE$_r$ at this location. We discuss the variation of the phase relationship in a later paragraph.

The nonlinear energy transfer should be tested locally; however, it is noted that the electrostatic potential is not a local but a spatially integrated parameter. Revisiting the momentum balance equation $\partial_t\tilde{U}_{\mathrm{SE}_r}=-\partial_r\langle\tilde{u}_r\tilde{u}_\theta\rangle-\mu\tilde{U}_{\mathrm{SE}_r}$, the local nonlinear energy transfer between the DW and SE$_r$ can be tested by the cross bispectrum $\langle\tilde{E}_\theta\tilde{E}_r\tilde{E}^*_{\mathrm{SE}_r}\rangle$ with fine frequency resolution, as presented in Eq. (3) of Ref. 7. Figure 3 shows enlarged views of the transfer function $F(f_1)\equiv[k_r(f_1)+k_r(f_2)]\Im\langle\tilde{E}_\theta(f_1)\tilde{E}_r(f_2)\tilde{E}^*_{\mathrm{SE}_r}(f_3)\rangle$ at three different radial locations; here $F(f_1)$ denotes the rate of kinetic energy transfer from fluctuations with frequencies f_1 and f_2 into frequency f_3. The SE$_r$ frequency f_3 is selected as 366 Hz, and $f_3=f_1+f_2$ is satisfied. The positive sign means energy transfer from the RS of the DW into the SE$_r$, and negative sign indicates the opposite. Error estimation is based on the cross coherence in k_r measurement and cross bicoherence in $\langle\tilde{E}_\theta\tilde{E}_r\tilde{E}^*_{\mathrm{SE}_r}\rangle$ measurement (the number of observations used in ensemble average >400).

Figure 3 clearly demonstrates that the SE$_r$ exchange energy via the RS. In addition to this, two distinctive features are found in the energy exchange. First, the spectra demonstrate that the energy transfer directions are not unique in frequency. The energy exchange from one part of the DW spectrum to the other part, mediated by the SE$_r$, can occur. The spectral form of the DW in this experiment has a finite bandwidth (not a fully developed turbulence). Therefore, the nonlinear physics between the SE$_r$ and DW would be understood on the basis of the PMI in a spectrum of DW.[20,28] Detailed measurements of spectral shape dynamics of fluctuations along with flows are left as important challenges for clarifying deep physical processes of the PMI.

The other discovery is that the energy input to the SE$_r$ by the RS can change sign depending on the radial location. The energy transfer intensities and directions are not unique with

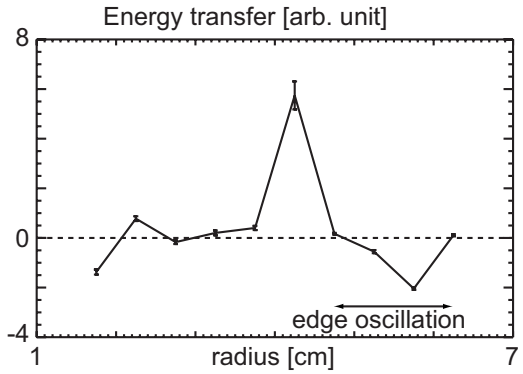

FIG. 4. Radial profile of total energy transfer rates to the SE_r.

radius. We obtained the total energy transfer rates by integration within the bandwidths of the DW (4–40 kHz) and SE_r (0.3–0.5 Hz). Figure 4 shows the radial profile of the total energy transfer rates $\int df_3 \int df_1 F(f_1)$. Definition of signs in Fig. 4 is the same as that in Fig. 3. The DW drives the SE_r significantly at $r=2.25$ and 4.25 cm. At the zero $k_r^{SE_r}$ location, energy transfer intensity is much smaller than in other locations. This is natural because the SE_r is weak at the location where $k_r \sim 0$. The SE_r is damped by the DW in some locations. This observation suggests a nonlocal energy transfer of fluctuations via the SE_r. The nonlocal transfer is possible in a recent theoretical prediction that the zonal flow could transmit the refractive force by which the spectral shape of turbulence is transformed and thus wave momentum can be enhanced.[21] The results of Fig. 4, the existence of the DW refraction by the SE_r, at the location of $k_r^{SE_r} \sim 0$ [see also Fig. 2(b)] suggest a picture in which the DW spectrum drives the SE_r at $r \sim 2$ and 4 cm and that the SE_r refracts the DW energy toward the $r \sim 3$ cm location where the SE_r is damped.

We compare the driving force with the damping force on the SE_r. The parameter in Ref. 29 is close to the present experiment. Thus we quote the estimation of ion-neutral collision as $\nu_{i0} \sim 6 \times 10^3$ s^{-1}. On the contrary, evaluation of the ion-ion collision frequency suggests that magnetization condition of our plasma is marginal. We may estimate the step size during the ion-ion collision at the ion gyroradius or ion mean free path. Using observed parameters,[25] the viscous damping by ion-ion collision is in the range of $\sim 500-25\,000$ s^{-1}. The damping rate composed of the neutral drag and ion-ion viscosity $(\nu_{i0}+\mu_{ii}q_{SE_r}^2) \times \int df_3 |\tilde{E}_{SE_r}(f_3)/B|^2$ at $r=4.25$ cm is less than or close to 2–3 (arbitrary unit, the same unit as that in Fig. 4). In this rough estimation, the driving force by the RS exceeds the damping force at the peak of the drive. Precise quantitative estimation of damping rate and consideration of nonlinear saturation of SE_r (Ref. 28) are necessary for understanding the discrepancy between driving and damping forces in future work.

In conclusion, we observed the PMI instability between the DW fluctuation and the sheared radial electric field structure in a cylindrical laboratory plasma. The modulation of the radial wave number of the DW is confirmed, and oscillation of the RS per mass density of DW spectrum is correlated with the sheared radial electric field oscillation. Nonlinear energy transfer rates show excitation of the sheared radial electric field by the DW at the location where the sheared radial electric field has finite radial wave numbers. The change of the energy transfer direction in spectral and real spaces is discovered, indicating a nonlocal energy transfer of fluctuations via channel of the sheared radial electric field.

We are grateful to Professor T. Ohkawa and Professor F. Wagner for useful discussions. This work was partially supported by Grant-in-Aids for SPR (Grant No. 16002005) (Itoh project) and for YS (B) (Grant No. 18760637) of MEXT, Japan, and by the collaborations of NIFS (Grant No. NIFS07KOAP017), RIAM of Kyushu University, and The University of Tokyo. We also appreciate the experimental supports of Mr. T. Nishizima, Mr. M. Kawagughi, and Dr. K. Kamataki.

[1] A. Yoshizawa, S.-I. Itoh, and K. Itoh, *Plasma and Fluid Turbulence: Theory and Modelling* (Institute of Physics, Bristol, 2003).
[2] P. Diamond, S.-I. Itoh, K. Itoh, and T. Hahm, Plasma Phys. Controlled Fusion **47**, R35 (2005).
[3] M. Rosenbluth and F. Hinton, Phys. Rev. Lett. **80**, 724 (1998).
[4] N. Winsor, J. Johnson, and J. Dawson, Phys. Fluids **11**, 2448 (1968).
[5] Z. Lin, T. S. Hahm, W. W. Lee *et al.*, Science **281**, 1835 (1998).
[6] P. Diamond, M. Rosenbluth, E. Sanchez *et al.*, Phys. Rev. Lett. **84**, 4842 (2000).
[7] G. Tynan, R. Moyer, M. Burin *et al.*, Phys. Plasmas **8**, 2691 (2001).
[8] A. Fujisawa, K. Itoh, H. Iguchi *et al.*, Phys. Rev. Lett. **93**, 165002 (2004).
[9] A. Fujisawa, K. Itoh, A. Shimizu *et al.*, Phys. Rev. Lett. **98**, 165001 (2007).
[10] A. Fujisawa, A. Shimizu, H. Nakano *et al.*, Plasma Phys. Controlled Fusion **49**, 211 (2007).
[11] A. Fujisawa, A. Shimizu, H. Nakano *et al.*, J. Phys. Soc. Jpn. **76**, 033501 (2007).
[12] H. Xia and M. Shats, Phys. Rev. Lett. **91**, 155001 (2003).
[13] M. Shats, W. Solomon, and H. Xia, Phys. Rev. Lett. **90**, 125002 (2003).
[14] D. Gupta, R. Fonck, G. McKee *et al.*, Phys. Rev. Lett. **97**, 125002 (2006).
[15] V. Sokolov, X. Wei, A. Sen *et al.*, Plasma Phys. Controlled Fusion **48**, S111 (2006).
[16] C. Holland, J. Yu, A. James *et al.*, Phys. Rev. Lett. **96**, 195002 (2006).
[17] M. Shats and W. Solomon, New J. Phys. **4**, 30 (2002).
[18] T. Yamada, S.-I. Itoh, T. Maruta *et al.*, Nat. Phys. **4**, 721 (2008).
[19] Y. Nagashima, K. Hoshino, A. Ejiri *et al.*, Phys. Rev. Lett. **95**, 095002 (2005).
[20] P. Diamond, M. Rosenbluth, F. Hinton *et al.*, Plasma Physics and Controlled Nuclear Fusion Research Report No. IAEA-CN-69/TH3/1, 1998.
[21] P. Diamond, C. McDevitt, O. Gurcan *et al.*, Phys. Plasmas **15**, 012303 (2008).
[22] C. Holland, G. Tynan, R. Fonck *et al.*, Phys. Plasmas **14**, 056112 (2007).
[23] P. Manz, M. Ramisch, U. Stroth *et al.*, Plasma Phys. Controlled Fusion **50**, 035008 (2008).
[24] Y. Nagashima, S.-I. Itoh, S. Shinohara *et al.*, Plasma Fusion Res. **3**, 056 (2008).
[25] Y. Saitou, A. Yonesu, S. Shinohara *et al.*, Phys. Plasmas **14**, 072301 (2007).
[26] Y. Nagashima, S.-I. Itoh, S. Shinohara *et al.*, J. Phys. Soc. Jpn. **77**, 114501 (2008).
[27] L. Chen, R. B. White, and F. Zonca, Phys. Rev. Lett. **92**, 075004 (2004).
[28] K. Itoh, N. Nagashima, S.-I. Itoh *et al.*, Phys. Plasmas **12**, 062303 (2005).
[29] G. Tynan, C. Holland, J. Yu *et al.*, Plasma Phys. Controlled Fusion **48**, S51 (2006).